Supplementary Information

Electrostatically hindered diffusion for predictable release of encapsulated cationic antimicrobials

Viktor Eriksson[a], Erik Nygren[b], Romain Bordes[a], Lars Evenäs[a], and Markus Andersson Trojer[a,c,*]

[a] Department of Chemistry and Chemical Engineering, Chalmers University of Technology, Gothenburg, Sweden

[b] RISE Research Institutes of Sweden, Department of Bioeconomy and Health, Gothenburg, Sweden

[c] RISE Research Institutes of Sweden, Department of Materials and Production, Mölndal, Sweden

[*] Corresponding author. E-mail address: markus.andersson-trojer@ri.se

1 Experimental

1.1 PLGA acid value

The number of carboxylic acid end groups in the PLGA was determined by potentiometric titration as described elsewhere.[1]

1.2 Microsphere size distribution

Using optical micrographs, the size distributions of formulated microsphere batches were estimated. The micrographs were processed in ImageJ (National Institute of Health) to yield the individual areas of at least 800 particles, assumed to be perfect spheres. The radii of the microspheres were then fitted to a log-normal size distribution.

$$P(r, M, S) = \frac{1}{S\, r\sqrt{2\pi}} \exp\left(- \frac{(\ln(r) - M)^2}{2S^2} \right) \quad r > 0 \tag{S1}$$

Here, M and S is the mean and standard deviation, respectively, of the logarithmized radius r. The mean, μ, and standard deviation, σ, of the size distribution can then be calculated as

$$\mu = \exp\left(M + \frac{S^2}{2} \right) \tag{S2}$$

and

$$\sigma = \sqrt{\exp\left(2M + S^2\right)\left(\exp\left(S^2\right) - 1\right)}. \tag{S3}$$

1.3 Infrared spectroscopy

To evaluate the fraction of bound and unbound OCT in the prepared PLGA films, deconvolutions of the absorption band at around 1660 cm^{-1} were performed. Peaks were fitted as Gaussian peaks,

$$f(x) = a \exp\left(- \frac{(x - b)^2}{2c^2} \right) + y_0, \tag{S4}$$

where a is the amplitude of the peak, b is the position of the peak center, and c controls the peak width. The spectrum of the pure PLGA film was subtracted from the three OCT-loaded films. Recorded spectra were fitted with two individual Gaussian peaks centered at 1651 and 1656 cm^{-1}. The width of each of the two peaks was fitted globally to all the three spectra, whereas the amplitudes were fitted individually to each spectrum. A baseline y_0 was also applied and fitted.

The bound OCT-fraction was calculated by comparing the area of the fitted peak corresponding to bound OCT at 1656 cm^{-1} to the sum of the fitted peaks.

1.4 Release measurements

The final stage of release the release or sorption measurements presented in the main article is controlled by the degradation of the polymer matrix, rather than a restricted diffusivity of OCT. Since the hydrolysis of PLGA in a small microcapsule occurs via bulk degradation[2], an excess of water was assumed in the microcapsules. In addition to water, the hydrolysis is catalyzed by acid, and thus becomes autocatalyzed by the carboxylate formation during degradation. Starting with release and sorption measurements in media containing Brij L23, the degradation for these systems was assumed to follow pseudo-first order kinetics.[3] During degradation, the formed oligomeric PLGA fragments were released and solubilized in the aqueous phase which led to a negligible increase in acid groups. This degradation was described as

$$f_{d1}(t) = \left(1 - \frac{\alpha}{1+\alpha}\right)\left(1 - \exp\left(-k_{d1}t\right)\right), \tag{S5}$$

where k_{d1} is the apparent rate constant for the pseudo-first order degradation reaction.

For release and sorption media without any solubilizing agents, the generated acid groups remained inside the microcapsules. This would induce an autocatalytic degradation behavior, which has been modeled by Antheunis et al.[4] using the rate law

$$\frac{du}{dt} = k_{d2}\left([E]_0 - u\right)\left([A]_0 + u\right). \tag{S6}$$

Here, u is the concentration of carboxylic acid groups, $[E]_0$ and $[A]_0$ are the initial concentrations of ester bonds and acid, respectively, and k_{d2} is a second order apparent rate constant. The solution to this equation is given by

$$u(t) = [A]_0 \frac{\exp\left(c_1 t\right) - 1}{1 + c_2 \exp(c_1 t)} \tag{S7}$$

with the coefficients c_1 and c_2 defined as

$$c_1 = \left([E]_0 + [A]_0\right)k_{d2} \tag{S8}$$

$$c_2 = \frac{[A]_0}{[E]_0} \tag{S9}$$

Here, the extent of degradation (amount of generated acid) was assumed to be proportional to the fractional release of OCT. Thus, to arrive at the fractional release of OCT, Equation (S6) must be scaled according to

$$f_{d2}(t) = \frac{\alpha}{1+\alpha} + \left(1 - \frac{\alpha}{1+\alpha}\right)\frac{u(t)}{[E]_0} \quad \text{(S10)}$$

Finally, the rate expressions in Equation (S5) or Equation (S10) could be combined with the diffusion-controlled release (Equation (6) as described in the main article) to yield an expression for the overall observed release,

$$f_{release}(D,t) = f_0 + p_b f_b(t) + (1 - p_b) f_{pd}(D,t) + f_{di}(t). \quad \text{(S11)}$$

2 Results

2.1 PLGA acid value

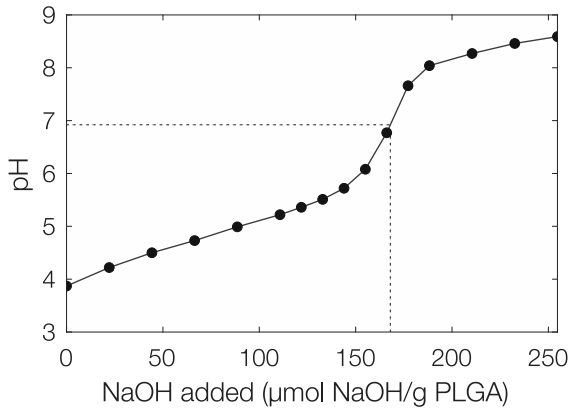

Fig. S1. Acid value of PLGA from titration with aqueous NaOH.

2.2 Microsphere formulation

The size distribution of prepared microspheres with or without OCT is shown in Fig. S2. Since the microsphere formulation is preceded by creating a DCM-in-water emulsion, the interfacial tension between DCM determines the size of emulsion droplets, and subsequent microspheres. The surface activity of OCT likely reduces this interfacial tension efficiently, leading to a narrower size distribution shifted towards smaller radii for OCT-loaded microspheres compared to microspheres without any active (Fig. S2).

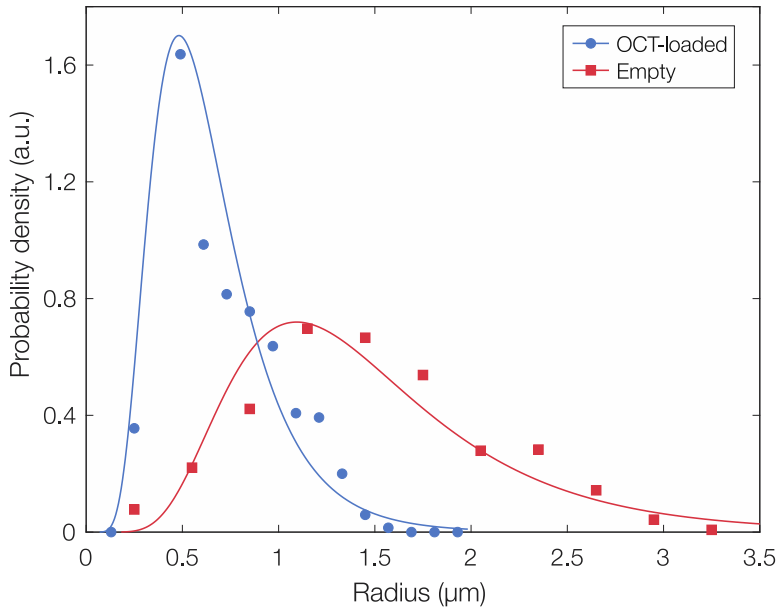

Fig. S2. Size distributions for the PLGA microspheres loaded with 5 % OCT, and empty microspheres without OCT.

Table S1. Fitted size distribution parameters with 95 % confidence intervals for the OCT-loaded and empty microspheres.

	μ (μm)	σ (μm)
OCT-loaded	0.65 ± 0.02	0.3 ±0.1
Empty	1.50 ± 0.06	0.72 ± 0.3

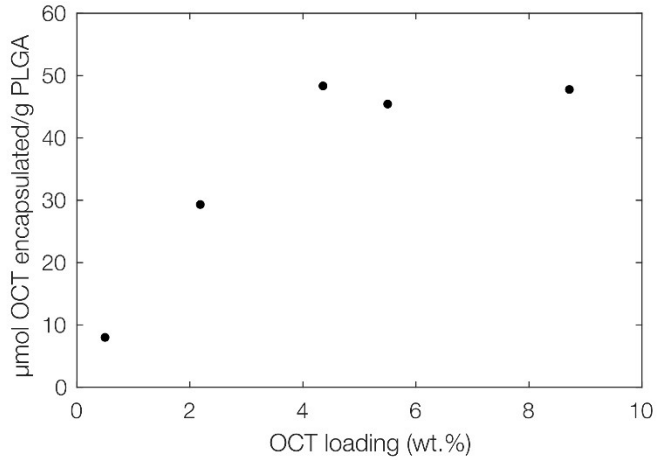

Fig. S3. Encapsulated amount of OCT as a function of the initial loading of OCT in the microcapsule during formulation.

In Fig. S4 the encapsulated fraction of OCT is shown for two kinds of PLGA with either a lactic:glycolic-ratio of 70:30 (Polysciences) or 50:50 (Evonik) and with either free carboxylic acid (A) or ester capped end groups. As can be seen, the encapsulation yield is rather independent on the polymer hydrophilicity (lactic:glycolic ratio), but to a great extent dependent on whether there are free acid end groups available or not to bind OCT.

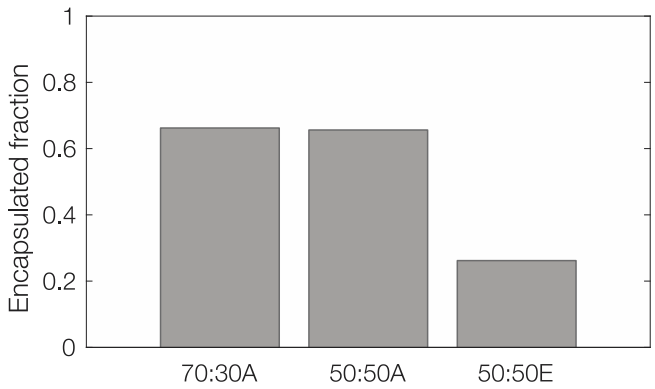

Fig. S4. Encapsulated OCT fraction at a loading of 5% in three different grades of PLGA with a lactic:glycolic ratio of either 70:30 or 50:50, and with either free carboxylic acid (A) or ester capped (E) end groups.

2.3 Infrared spectroscopy

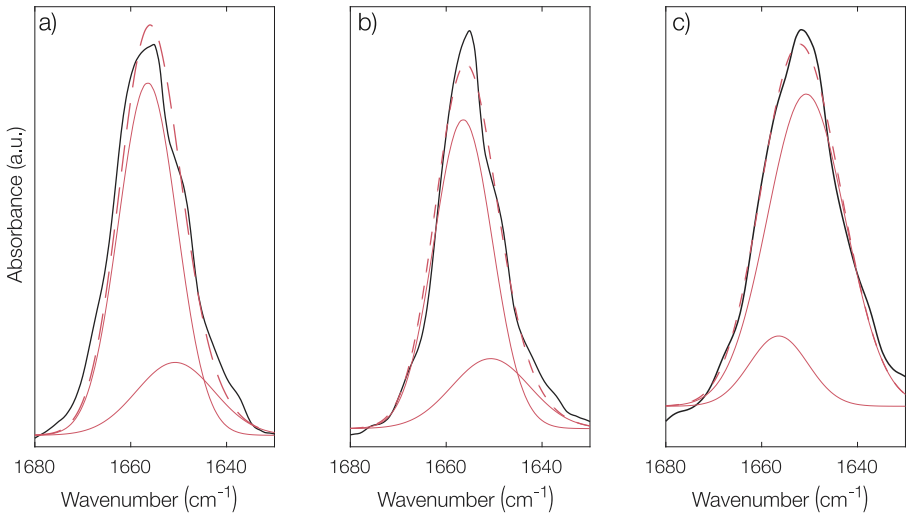

Fig. S5. Deconvolutions of the absorption band around 1660 cm^{-1} for PLGA films containing a) 2%, b) 5%, and c) 10 % OCT. In the figure, recorded spectra (—), fitted Gaussian peaks (—) and the sum of fitted peaks (- - -) are shown.

Table S2. Fraction of bound OCT from deconvolution for OCT-loaded films.

OCT loading (%)	Bound fraction (%)
2	86
5	80
10	13

2.4 UV-vis spectrophotometry

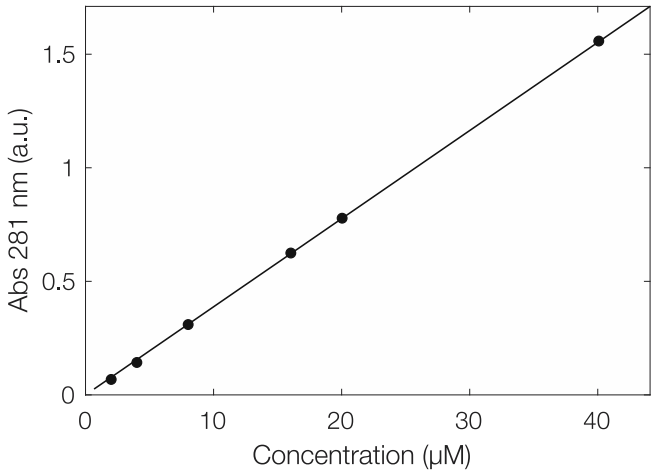

Fig. S6. UV-vis calibration curve for OCT with a fitted absorption coefficient of $\varepsilon = 38.8 \pm 0.4$ $mM^{-1}cm^{-1}$.

2.5 Release measurements

In addition to the diffusion-controlled release for the first part of the release and sorption measurements presented in the main article, the final part of the release was controlled by the polymer degradation kinetics with apparent rate constants shown in Fig. S7. As motivated previously, either a pseudo-first order rate expression (for measurements in media containing Brij L23) or a modified second order rate expression (for measurements in media without Brij L23) was used. In all cases, the models were well-fitted to the experimental data as seen by the dotted lines in Fig. 3-5 in the main article as well as the individually fitted data in Fig. S8 and Fig. S9. Starting with the release measurements, a fourfold increase in k_{d1} and a twofold increase in k_{d2} was observed upon increasing the temperature from 22 °C to 37 °C. For the corresponding sorption measurements, the trends were identical with increasing rate constants at increasing temperatures, however, there was a slight difference in their absolute values.

The origin of this difference between release and sorption remains unclear, but it might be linked to a difference in spatial distribution of OCT within the microcapsules. For release measurements, OCT was initially uniformly distributed in the microcapsules. In the case of sorption, however, it is possible that OCT only had sufficient time to reach the outermost parts of the microcapsule by diffusion before being released again by degradation. In this outermost region, it is possible that OCT was more sensitive to the PLGA degradation and consequently was released at a faster rate (resulting in an apparent increase of the degradation rate constants).

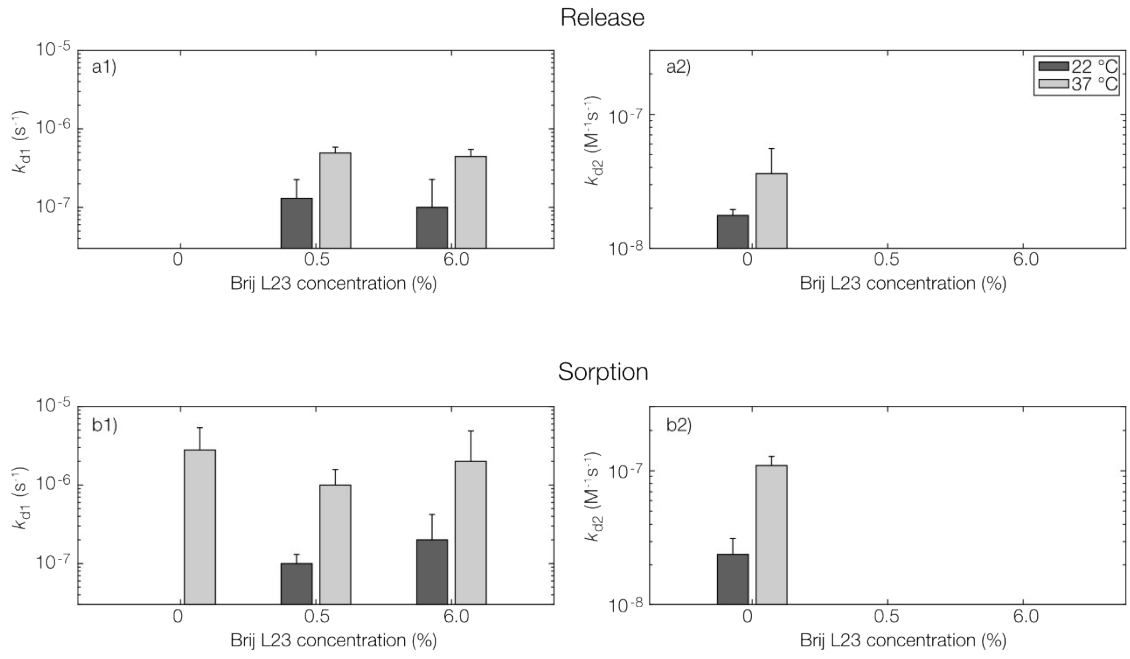

Fig. S7. Fitted a1) first order and a2) second order rate constants from release measurements. b) Corresponding values for the sorption measurements. Values are presented with a 95% confidence interval for the fitted parameters. The legend is valid for all subfigures.

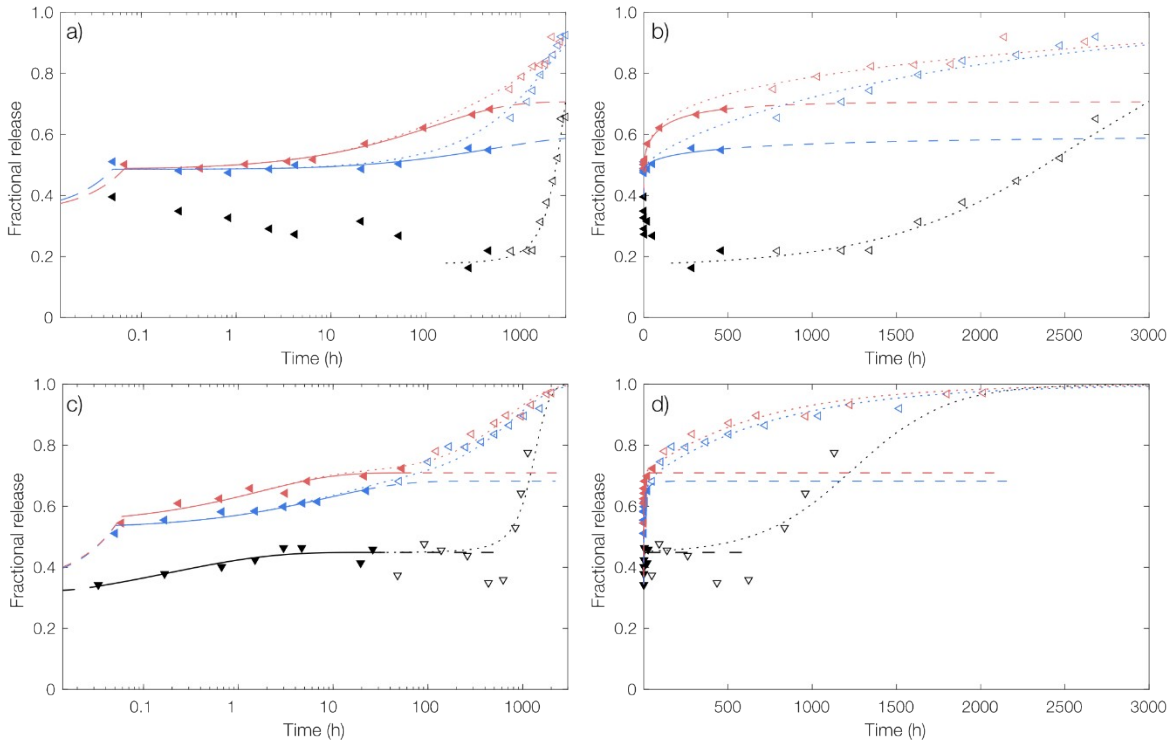

Fig. S8. Release of OCT from PLGA microspheres in TRIS-buffered release media at pH 7.4 with 0% (—), 0.5% (—), and 6% (—) Brij L23. Measurements were performed at a) 22 °C and c) 37 °C and are shown both on a logarithmic time scale, a) and c), and a linear time scale, b) and d). Experimental data is shown along with individually fitted diffusion models to each data set.

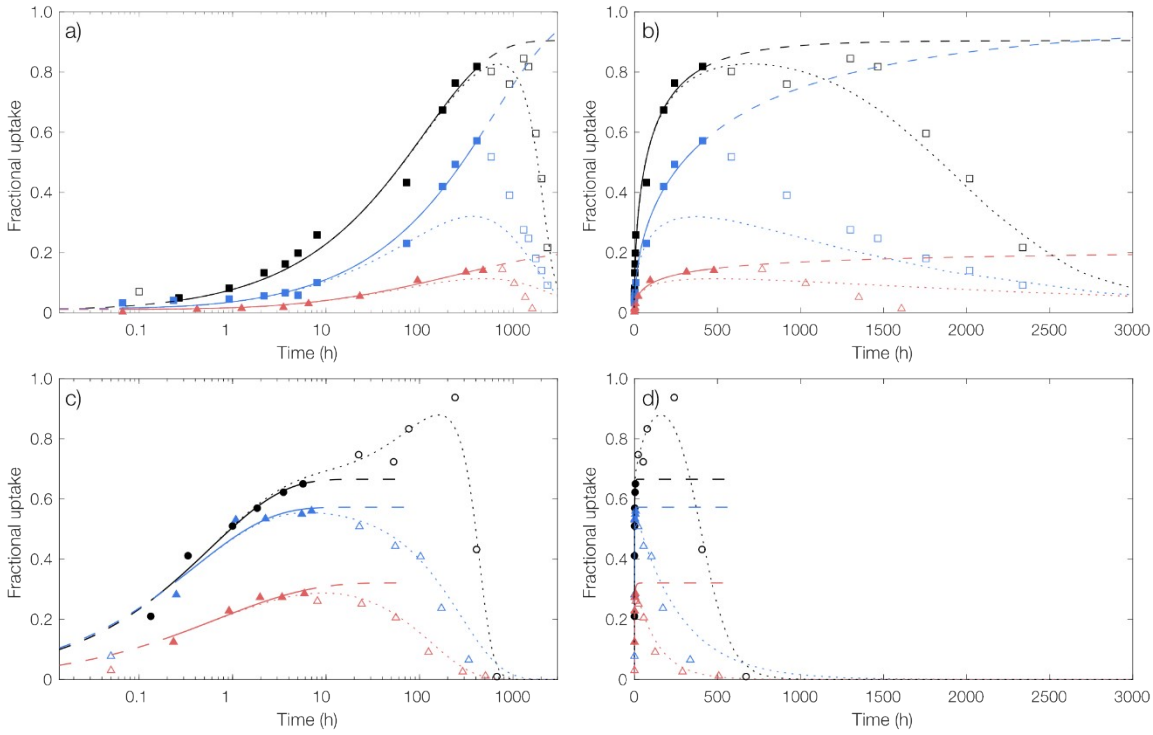

Fig. S9. Sorption of OCT from TRIS-buffered aqueous phases containing 0% (—), 0.5% (—), and 6% (—) Brij L23 at pH 7.4 into empty PLGA microspheres at a) 22 °C and b) 37 °C. The data is shown both on a logarithmic time scale, a) and c), and a linear time scale, c) and d). Experimental data is shown along with individually fitted diffusion models to each data set.

Table S3. Individually fitted diffusion (D_i) and partition (K_i) coefficients and release burst fractions for release and sorption studies in aqueous media with different concentrations of solubilizing Brij L23 at 22 °C and 37 °C along with k_I calculated from fitted $D_{release}$ and $D_{sorption}$. Values are presented with a 95% confidence interval for the fitted parameters.

22 °C						
Brij L23 fraction (%)	Burst fraction	$D_{release}\cdot10^{20}$ (m^2/s)	$K_{release}\cdot10^{-3}$	$D_{sorption}\cdot10^{19}$ (m^2/s)	$K_{sorption}\cdot10^{-3}$	k_I
0	-	-	-	5.9±2.8	0.3±0.5	-
0.5	0.14±0.18	1.3±7.9	3.4±3.2	1.3±0.6	0.1±1.3	0.1
6.0	0.14±0.01	7.5±5.8	1.8±0.4	0.2±0.2	12.1±4.0	0.28
37 °C						
Brij L23 fraction (%)	Burst fraction	$D_{release}\cdot10^{20}$ (m^2/s)	$K_{release}\cdot10^{-3}$	$D_{sorption}\cdot10^{19}$ (m^2/s)	$K_{sorption}\cdot10^{-3}$	k_I
0	0±0.06	14.8±38.8	5.4±0.7	7.6±4.5	1.6 ±0.6	0.19
0.5	0.19±0.08	1.0±2.8	2.1±1.2	9.0±10.0	2.4±1.0	0.01
6.0	0.20±0.06	5.2±8.7	1.8±0.4	1.9±2.2	6.9±2.7	0.27

As seen by the fit in Fig. S8 and as discussed in the main text, there is a lack of data points to confidently fit these data series individually which is evidenced by large uncertainties in the fitted parameters. Because of this, there are also significant uncertainties and deviations in the

calculated k_I-values based on individual fits of D. Additionally, it should be emphasized that this is the best fit with all parameters free.

2.5.1 The PLGA-OCT interaction

The interaction between PLGA and OCT can be considered as a reversible binding event,

$$A_{free} + S \rightleftharpoons A_{bound}$$

where the substance A either is free or bound to specific adsorption sites S. The equilibrium constant for this reversible reaction can then be expressed as

$$k_I^{eq} = \frac{[A_{bound}]}{\Gamma_{max}[A_{free}]} \tag{S12}$$

with Γ_{max} being the number of free binding sites in the material. By defining $[A_{bound}]=\Gamma = c$ and c_0 as the total concentration of A, k_I^{eq} can then be expressed as

$$k_I^{eq} = \frac{c}{(\Gamma_{max} - c)(c_0 - c)}. \tag{S13}$$

By adding $(c_0-c)/(c_0-c)=1$ to both sides, we get

$$k_I^{eq}(\Gamma_{max} - c) + 1 = \frac{c}{c_0 - c} + \frac{c_0 - c}{c_0 - c} = \frac{c_0}{c_0 - c}. \tag{S14}$$

It can clearly be seen that the right-hand side of the equation is the inverse of the free fraction of A, defined as k_I in the article. Hence, we get

$$k_I = \frac{c_0 - c}{c_0} = \frac{1}{k_I^{eq}(\Gamma_{max} - c) + 1} \tag{S15}$$

This indicates that k_I is concentration-dependent since c depends on the initial starting conditions c_0 according to Equation (S13). A closer inspection of this relation shows that the strong concentration dependence commences as c_0 surpasses Γ_{max}, shown in Fig. S9.

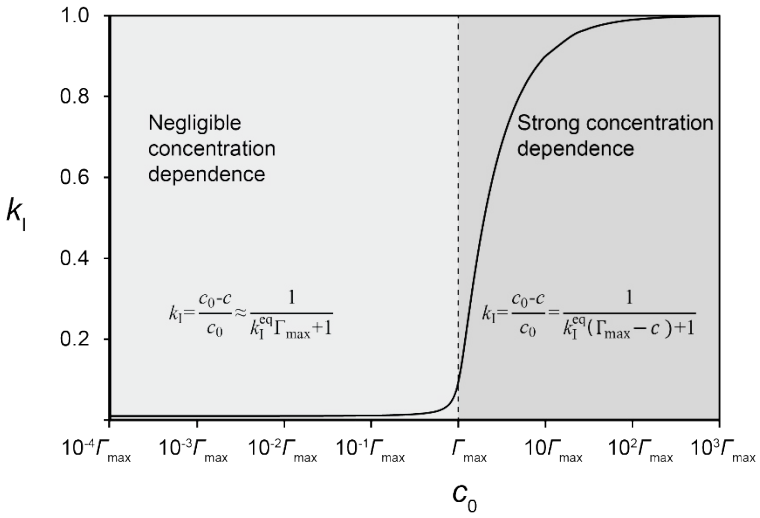

Fig. S10. The free fraction k_I as a function of the total amount c_0 in the capsule. The concentration is expressed in units of Γ_{max}. In this example, the product $k_I^{eq}\Gamma_{max}$ is arbitrarily set to 100.

On the other hand, as c_0 falls below Γ_{max}, k_I drops quickly to the value given by the reduced equation

$$k_I = \frac{c_0 - c}{c_0} = \frac{1}{k_I^{eq}\Gamma_{max} + 1}. \quad \text{(S16)}$$

We must now recognize that as the encapsulation of OCT as presented in the article is limited by Γ_{max}, c_0 will always be lower than Γ_{max}. In addition, during the course of the release event, k_I will approach the asymptotic k_I value given by Equation (S16). If we use the data provided in the article indicating that a maximum of two thirds of the available sorption sites are occupied, the total error cannot exceed a scaling factor of 1.1 in the limit as $k_I^{eq \to \infty}$. Hence, for a system - such as the one presented in the article – where the encapsulation is limited by the binding event, Equation (S16) provides a very good approximation of the bound fraction during the entire release event.

3 References

1. J. K. Y. Hong and S. P. Schwendeman, *Biomacromolecules*, 2020, **21**, 4087-4093.
2. F. v. Burkersroda, L. Schedl and A. Göpferich, *Biomaterials*, 2002, **23**, 4221-4231.
3. A. N. Ford Versypt, D. W. Pack and R. D. Braatz, *Journal of Controlled Release*, 2013, **165**, 29-37.
4. H. Antheunis, J.-C. van der Meer, M. de Geus, A. Heise and C. E. Koning, *Biomacromolecules*, 2010, **11**, 1118-1124.